

## Nucleation and Condensation in the Primitive Solar Nebula

A. G. W. CAMERON AND M. B. FEGLEY

*Harvard-Smithsonian Center for Astrophysics, Cambridge, Massachusetts 02138*

Received March 5, 1982; revised June 4, 1982

Using the accretion disk physics of Lynden-Bell and Pringle, we constructed a section of a model of the primitive solar nebula, subject to the assumption that the optically thick part of the disk is convective and isentropic and that there is a steady mass flow toward the axis of the disk at the rate of  $10^{-5}$  solar masses per year. The properties of the model support these assumptions. We studied that portion of the disk which includes the interface between the region where high-temperature solid condensates can exist and where they will be totally evaporated. The total evaporation front separating these two regions rises vertically off the midplane and then curves overhead inward for a long distance before emerging through the photosphere. We applied Salpeter's modification of classical condensation theory to study the nucleation and condensation of materials in gas that moves through the total evaporation front in the direction of lower temperatures. We conclude that a very substantial supercooling of the vapors is required before nucleation can take place, but the great uncertainties in the surface energies of the condensation products render the point of nucleation highly uncertain. It is probable that several materials have become unstable against condensation by the time that nucleation can take place, so that the formation and growth of condensate nuclei is likely to be a very complex process.

### INTRODUCTION

The primitive solar nebula may be modeled using the frictionally induced transport theory of Lynden-Bell and Pringle (1974) [see Cameron (1978) and Lin and Papanoizou (1980)] if the principal frictional mechanism within the nebula is turbulent viscosity, or that plus other sources of viscosity which can be included within the modeling. The primitive solar nebula is formed at the center of a collapsing interstellar gas cloud fragment, and it is probable that the internal transport time scales for energy, angular momentum, and mass within the bulk of the nebula become adjusted to comparability with the infall time scale (about  $10^5$  years) throughout the bulk of the nebula through the establishment of a steady-state mass distribution within the nebula (the only alternative is the unlikely condition that the internal time scales should be longer than the infall time scale). Subject to these approximations the nebula evolves in the expected way: mass flows outward near the outer edge and inward

near the center; angular momentum always flows outward; and the gravitational energy which is released flows outward and is also locally dissipated (Cameron, 1978). This dissipation is responsible for heating the nebula; throughout the infall period the mass of the Sun grows and the temperature in any region of planetary formation (by which we mean at a variable radial distance at which the specific angular momentum is conserved) will continually increase.

We constructed a model of a section of the primitive solar nebula in order to study nucleation and condensation processes within it. This construction involves a relatively simple application of the Lynden-Bell and Pringle theory subject to steady mass flow conditions.

The interstellar gas infalling into the solar nebula contains condensed matter in the form of interstellar grains, initially at very low temperatures (5 to 10°K). As such grains move into warmer regions of the gas, the more volatile constituents evaporate. Turbulent motions within the gas actually cause a diffusion of the grains, as has re-

cently been emphasized by Morfill (1981), so that layers of molecules of intermediate volatility are likely to condense and again evaporate as the grains diffuse. However, when a parcel of the gas moves into a region with a temperature above about 1600°K, the grains will become completely evaporated. We refer to the surface within the nebula containing critical combinations of temperature and pressure at which this total evaporation occurs as "the total evaporation front." In this paper we have taken the evaporation of corundum to define this total evaporation front; we have thus neglected the somewhat greater stability of certain refractory heavy metals, such as osmium, which we address later.

In the outer part of the nebula, when a parcel of gas moves in such a way as to undergo expansion with cooling, there are always large numbers of grains present which can act as condensation centers for any vapors that become supersaturated. However, in the inner solar nebula within the total evaporation front, no nucleation centers are present. Such centers can only be created by statistical fluctuations in molecular clustering within the gas, and this generally requires a high degree of supersaturation, as Blander and Katz (1967) have long argued.

At pressures below  $10^{-2.7}$  bars, which will always be the case for the conditions considered in this paper, according to chemical equilibrium calculations, the first condensate should be corundum ( $\text{Al}_2\text{O}_3$ ). Hibonite ( $\text{CaAl}_{12}\text{O}_{19}$ ) should condense only a few degrees below corundum (Fegley, 1982).

We applied a modification of classical nucleation theory due to Salpeter (1974) to estimate the degree of supersaturation needed to create condensation centers when a parcel of gas moves through the total evaporation front toward lower temperatures. Using surface energies appropriate to refractory phases, the formal result is that the gas must become supercooled by several hundred degrees Kelvin in order to

form condensation centers. We discuss some of the implications of this result.

#### THE MODEL CONSTRUCTION

In Cameron (1978), models of the primitive solar nebula were constructed with an isothermal vertical temperature profile, partly for computational convenience, and partly because large-scale turbulent velocities were taken sufficiently close to sound speed so that mechanical wave generation was considered likely to play a substantial role in heating the upper layers of the atmosphere in the disk. The attempt at that time was to go to one extreme of assumptions in order to see if gravitational instabilities in the disk could be avoided. It was concluded that such instabilities could not be avoided. However, if less extreme turbulent velocities are assumed, then the efficiency of heating by mechanical energy deposition in the upper atmosphere should be greatly reduced, and it is better to neglect that heating and to assume that the optically thick parts of the disk are isentropic. This is the approach that was taken by Lin and Papaloizou (1980). We also make that assumption here, although we are still taking the velocity of the largest eddies to be a substantial fraction (one-third) of sound speed.

In the present work we took a fairly simple approach to the construction of a segment of the primitive solar nebula centered around a midplane temperature of 1600°K. We assumed 0.5 solar masses of material to have collected into the protosun on the axis of the disk, thus looking at conditions half-way through the accumulation history of the Sun. We assumed a steady flow inward of mass at the rate of  $10^{-5}$  solar masses per year, consistent with the time scales in Cameron (1978). We assumed Keplerian motion within the disk, thus neglecting gravitational forces due to the mass of the disk itself. An analysis of accretion disks subject to these simple assumptions was included in Cameron (1978); in the following, equation numbers preceded by "C" refer to equations in that analysis.

The outward mass flow may be written in the form (C45)

$$F = -3\pi\nu\sigma, \quad (1)$$

where  $\nu$  is the turbulent viscosity and  $\sigma$  is the column surface density in the disk. The viscous couple between two adjacent concentric cylinders of matter is then (C44)

$$g = -F(GMR)^{1/2}, \quad (2)$$

where  $G$  is the gravitational constant,  $M$  is the central mass on the spin axis, and  $R$  is the radial distance. It may be seen that the assumptions of the problem define  $g$  everywhere.

Given the viscous couple and the local rate of shearing, the local rate of dissipation of energy per square-centimeter column is determined to be (C9)

$$D = \frac{1}{2\pi R} g \left[ -\frac{\partial\Omega}{\partial R} \right], \quad (3)$$

where  $\Omega$  is the angular (Keplerian) velocity given by (C40)

$$\Omega = \left[ \frac{GM}{R^3} \right]^{1/2}. \quad (4)$$

From Eq. (3), assuming that energy flows perpendicular to midplane, the photospheric temperature at each end of a square-centimeter column is (C10)

$$T_{\text{ph}} = \left[ \frac{D}{2\sigma_0} \right]^{1/4}, \quad (5)$$

where  $\sigma_0$  is the radiation constant. It may now be seen that the local photospheric temperature follows immediately from the assumption of the steady mass flow rate.

It remains to determine the local properties of the disk. The temperature given by Eq. (5) is the photospheric temperature and is assumed, for convenience, to be constant above the photosphere. Below the photosphere the gas is assumed to be isentropic. The opacity was taken to be the high opacity used by DeCampli and Cameron (1979) and shown in Fig. 1 of their paper. The grain opacities used were those supplied by

J. Pollack; it should be noted for later reference that there are some abrupt changes in Pollack's opacity values at temperatures of a few hundred degrees.

With the assumption that the turbulent viscosity resembles that of a molecular gas with isotropic properties, we write it in the form (C39)

$$\nu = \nu_0 c_s H, \quad (6)$$

where  $\nu_0$  is a constant coefficient here taken to be  $\frac{1}{3}$ , and  $c_s$  is the local sound speed at midplane, given by

$$c_s = \left[ \frac{\Gamma_1 N_0 k T_c}{\mu} \right]^{1/2}, \quad (7)$$

where  $\Gamma_1$  is the first adiabatic exponent,  $N_0$  is Avogadro's number,  $k$  is the Boltzmann constant,  $T_c$  is the temperature at midplane, and  $\mu$  is the mean molecular weight.  $H$  is the scale height for the largest turbulent eddies, taken to be

$$H = \sigma/\rho_c, \quad (8)$$

where  $\rho_c$  is the density at midplane.

It may thus be seen that the quantities  $\nu$  and  $\sigma$  in Eq. (1) are intimately linked together, and hence the column density  $\sigma$  can be determined iteratively from Eq. (1) if the structure of the column can be calculated. We calculated the column structure using the equation

$$\frac{dP}{dz} = -\frac{Gm\rho z}{(R^2 + z^2)^{3/2}}, \quad (9)$$

where  $P$  is the pressure in centimeter-gram-second units,  $z$  is the height above midplane, and  $\rho$  is the density. Equation (9) is more accurate than the thin-disk approximation that is usually used in disk structure calculations. Given the assumption that the pressure, temperature, and density gradients in the vertical direction are isentropic below the photosphere and isothermal above the photosphere, the machinery is in place for the calculation of the local disk structure everywhere in the disk where the

steady flow approximation is a reasonable one.

#### DETAILS OF THE MODEL DISK SEGMENT

We display a section of the disk between radial distances 0.4 and 1.4 AU. With half a solar mass on the spin axis, a body with the specific angular momentum of Mercury would be near a radial distance of 0.8 AU.

Figure 1 shows the height of the photosphere (in AU) and also the heights of the isotherms from 1000 to 1800°K, which are in the region of interest for the nucleation and condensation problem. It may be noted that there are some abrupt discontinuities in these curves; these discontinuities reflect the photospheric temperatures at which the Pollack grain opacities have abrupt changes. No physical significance should be associated with these discontinuities.

Figure 2 shows the pressures of the photosphere and midplane as a function of radial distance for the segment of the solar nebula. Also shown are the pressures of the various isothermal surfaces shown in Fig. 1. It should be noted that the pressures

along the isothermal surfaces increase with increasing radial distance. This means that the entropy of the gas decreases in the outward radial direction. Hence the gas is unstable against thermally driven convection in the radial direction. This provides a strong *a posteriori* justification for treating the gas isentropically within the photosphere in the calculation of the vertical column structure.

For a variety of substances the critical condensation temperature at which the condensing substances become marginally supersaturated in the gas phase can be written in the form

$$T = \frac{10^4}{(A - B \log P)}, \quad (10)$$

where  $P$  is the pressure in bars and  $A$  and  $B$  are constants determined by fitting thermodynamic data.

In the pressure range of interest to us, the first substance which becomes unstable against condensation is corundum ( $\text{Al}_2\text{O}_3$ ), for which  $A = 5.00671$  and  $B = 0.24558$ . Only a few degrees lower in temperature,

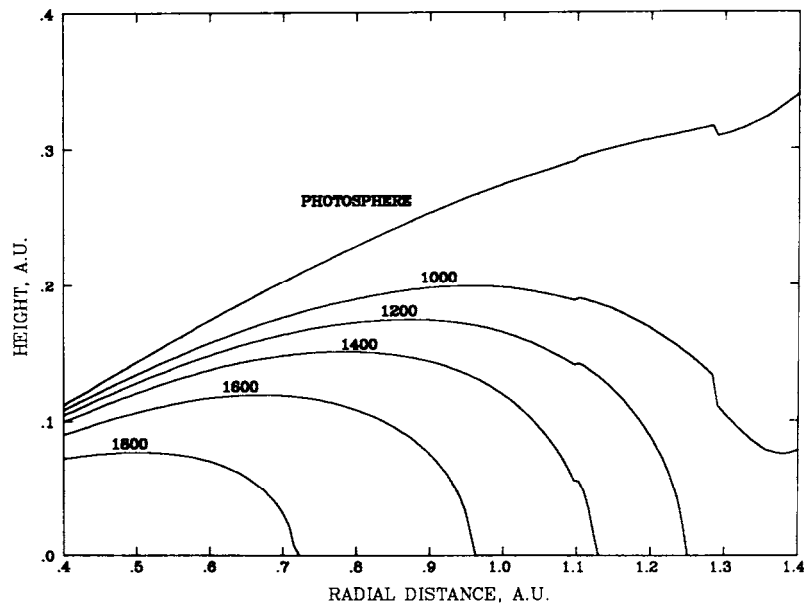


FIG. 1. The vertical structure of the solar nebula segment showing the heights of the photosphere and a number of isotherms. The vertical scale is slightly exaggerated relative to the horizontal scale.

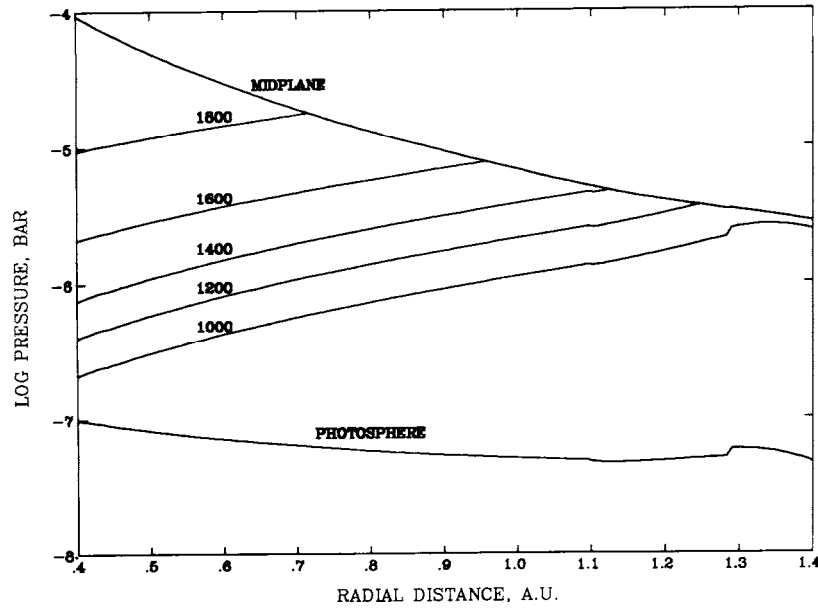


FIG. 2. The pressures at midplane and photosphere and for the selected isotherms of Fig. 1, as a function of radial distance in the solar nebula segment.

hibonite ( $\text{CaAl}_{12}\text{O}_{19}$ ), for which  $A = 4.7583$  and  $B = 0.34043$ , can in principle condense. Significantly lower are the condensation temperatures of the more abundant substances forsterite ( $\text{Mg}_2\text{SiO}_4$ ), for which  $A = 5.8216$  and  $B = 0.38327$ , and iron (as metal), for which  $A = 5.4541$  and  $B = 0.48342$ .

The condensation temperatures of these phases were calculated by standard methods which are described by Fegley (1980). Our condensation temperatures for corundum, forsterite, and iron are in excellent agreement with previous results, e.g., Trivedi and Larimer (1980). The condensation temperatures for hibonite are from Fegley (1982) and are the first results for this phase.

Figure 3 shows the position of the evaporation surfaces within the segment of the solar nebula. The line marked "evaporation front" is in fact what we call the total evaporation front at which corundum would evaporate, so that no condensed substances would be present at higher temperatures. This line is the evaporation front for corundum. The evaporation front for hi-

bonite is so close as to be essentially indistinguishable from that for corundum. The forsterite and iron curves lie at significantly greater heights and lower temperatures. It is interesting to note that condensed materials occupy the surface layers over a large range of radial distances for which the midplane is at a sufficiently high temperature to evaporate all condensed materials.

Figure 4 shows the temperatures of the photosphere and midplane and for the evaporation fronts within the selected segment of the primitive solar nebula. Figure 5 shows the pressures for the same quantities. Note that the pressure at the total evaporation front lies in the range  $10^{-5}$  to  $10^{-6}$  bars, and for the other substances the pressures are still lower. These pressures are significantly less than those usually assumed in condensation calculations for the primitive solar nebula.

It should be noted that the general features of Figs. 1 through 5 are rather insensitive to the precise assumptions made about the parameters that went into the calculation. With other parameters the total evap-

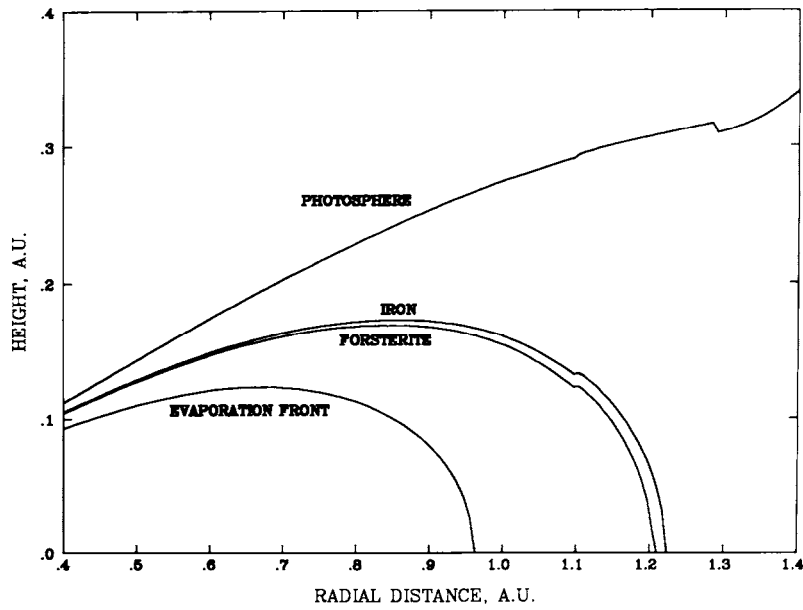


FIG. 3. The heights of the total evaporation front and of the evaporation fronts for forsterite and iron within the segment of the solar nebula.

oration front would be moved to somewhat greater or lesser distances, but the general characteristics of the solar nebula in the vicinity of this total evaporation front would be essentially the same. Thus a set of conditions similar to those shown in Figs. 1-5

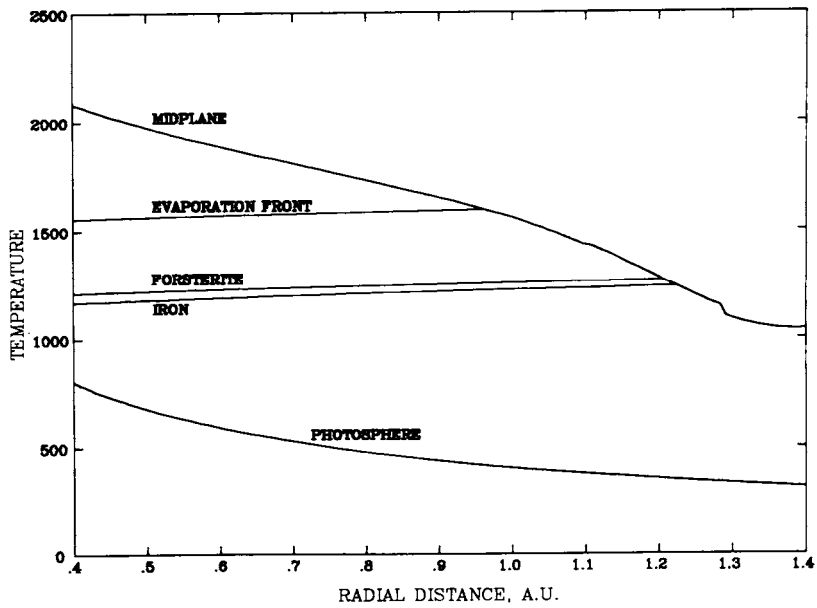


FIG. 4. The temperatures of the midplane, photosphere, and evaporation fronts as a function of radial distance within the segment of the solar nebula.

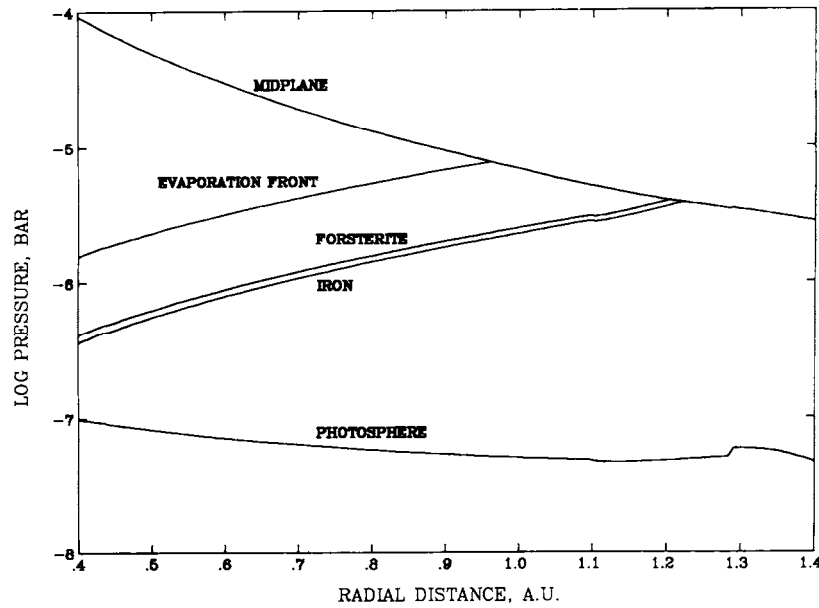


FIG. 5. The pressures of the midplane, photosphere, and the evaporation fronts as a function of the radial distance within the segment of the solar nebula.

should be present in the solar nebula, at some radial distance, throughout most of the history of the nebula.

#### NUCLEATION

Salpeter (1974) has pointed out that classical nucleation theory has been developed mainly for terrestrial experiments on liquid droplets held together by weak polarization forces. For the stellar atmospheres treated by Salpeter, and for the primitive solar nebula treated here, nucleation requires the formation of small crystals held together by strong valence forces. Salpeter made some modifications to classical nucleation theory to take these differences into account. He developed an expression for the temperature depression due to supercooling required for nucleation to take place, and he cast this expression in terms of the parameters of a rising and cooling gas current which is admirably suited for our own calculations. Draine and Salpeter (1977) have refined the treatment given by Salpeter (1974). However, these refinements are unnecessary for our purposes.

This temperature depression is given by the expression

$$\Delta T = \frac{TD_c}{B_{ph}} \left[ \frac{\alpha D_c}{kT \ln \eta} \right]^{1/2}, \quad (11)$$

where  $T$  is the normal bulk condensation (i.e., evaporation) temperature. Here  $\alpha$  is a complicated expression which may be approximated by unity, and  $D_c$  is related to the surface energy per surface molecule and is given by

$$D_c = \frac{8\pi}{3} E_s \left[ \frac{3}{4\pi n} \right]^{2/3}, \quad (12)$$

where  $n$  is the number density of the constituent molecules in the condensed phase and  $E_s$  is the surface energy of the solid. The quantity  $B_{ph}$  relates the condensation temperature to the partial pressure of the condensing substance and varies from about 40 to 60 times  $kT$  for refractory minerals such as corundum, hibonite, perovskite ( $\text{CaTiO}_3$ ), and gehlenite ( $\text{Ca}_2\text{Al}_2\text{SiO}_7$ ).  $B_{ph}$  for corundum is approximated by

$$B_{\text{ph}} = 55 kT. \quad (13)$$

The quantity  $\eta$  is the number of times an appropriate gas molecule sticks to a particular surface site on a droplet during the time required for  $\Delta T/T$  to increase by  $kT/B_{\text{ph}}$ . For corundum the critical gas molecule is metallic Al. Inserting this into Salpeter's expression for  $\eta$  and taking the sticking coefficient  $s$  as 0.1, we obtain

$$\eta = 3.8 \times 10^{-4} \frac{hP}{vT^{1/2}}, \quad (14)$$

where  $h$  is a pressure scale height given here by the minimum of  $0.5H$  or  $N_0kT/\mu g$ , where  $g$  is here the gravity,  $v$  is the gas streaming velocity in centimeters per second, and  $T$  and  $P$  are the gas temperature and pressure. Consistent with the value previously used for  $v_0$ , we take  $v$  to be one-third of sound speed.

The major uncertainty in the application of this theory to the primitive solar nebula is lack of precise knowledge of the surface energy  $E_s$  for corundum. Since there is considerable uncertainty in the theoretical and experimental determination of surface energies of refractory minerals and molten oxides and silicates, it is worth briefly reviewing the status of this area. Duga (1969) and Elliott *et al.* (1963) summarize surface energies for a large number of refractory solids and oxide and silicate melts, while Bruce (1965) presents a simple semiquantitative model for calculating surface energies from simple structural and thermodynamic considerations.

Several generalizations can be made upon examination of these extensive data. First, the surface energies of solids are expected to be about 10–20% larger than the surface energies of liquids (of the same composition) at the melting point (Adamson, 1967). Surface energies of slightly impure liquids, which may be formed by dissolving other cations in molten  $\text{Al}_2\text{O}_3$ , for example, will be even lower relative to the solid surface energies. However, we do not find the experimental data convincing in

this regard. The data for corundum and liquid  $\text{Al}_2\text{O}_3$ , as well as experimental data for other molten oxides and for molten and solid halides, do not generally show the expected 10–20% variation between liquid and solid surface energies. Second, the rather wide variations in solid surface energies obtained by different experimental and theoretical methods make the choice of surface energies for the nucleation calculations mildly exasperating. (Duga reports measured surface energies for corundum, which is a well-studied substance, from about 50 to 50,000 ergs/cm<sup>2</sup>, but each of these extremes is obviously grossly in error.) Third, the temperature and particle size dependences of the solid surface energies are difficult to measure and thus difficult to take account of in simple nucleation calculations. Keeping these caveats in mind, we took  $E_s$  for corundum to lie in the range 300–600 ergs/cm<sup>2</sup>. These values are representative of those obtained by various thermodynamic measurements such as heat of solution and dihedral angle measurements. They are also comparable to values calculated by Bruce (1965). However, the uncertainties are such that the  $E_s$  value for corundum might lie outside this range.

Figure 6 is a reproduction of Fig. 3 with the range of possible nucleation temperatures for corundum corresponding to the above-quoted uncertainty in the surface energy indicated by shading. The maximum temperature, corresponding to  $E_s = 300$  ergs/cm<sup>2</sup>, lies very close to the forsterite evaporation front. The minimum temperature, for  $E_s = 600$  ergs/cm<sup>2</sup>, lies below the photospheric temperature in the left half of the diagram, so that the shading has been terminated at the photosphere; it must be emphasized that it is not certain that nucleation would occur toward the left part of the diagram.

A referee has suggested that the homogeneous condensation of refractory trace metals such as osmium would provide nuclei for the heterogeneous condensation of corundum at its equilibrium condensation



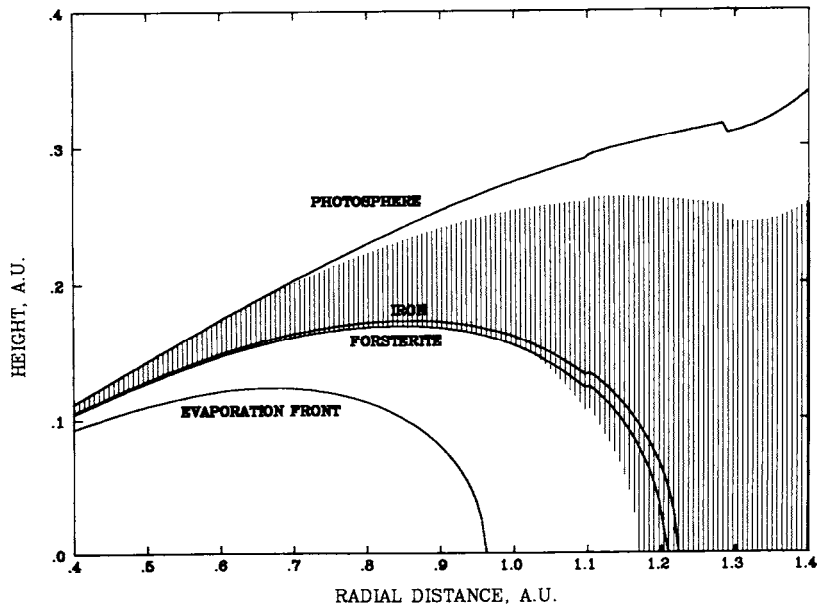


FIG. 6. The heights of the total evaporation front and of the evaporation fronts for forsterite and iron within the segment of the solar nebula. Overlain on the diagram, represented by shading, is the range of uncertainty in the nucleation temperature of corundum.

temperature. However, our calculations on Os nucleation indicate that large subcoolings occur. As a result Os(s) does not condense before corundum. The calculations were done using an  $E_s$  value for Os in the range of 1700–2000 ergs/cm<sup>2</sup>. These values are representative of  $E_s$  values for hexagonal close-packed (hcp) metals such as Co, Ti, and Os (Swalin, 1972).

Furthermore, if the refractory trace metals served as condensation nuclei for corundum or hibonite it might be expected that nuggets of refractory trace metals would be common in corundum or hibonite in high-temperature inclusions. Is this the case?

The literature reports of nuggets of refractory trace metals in inclusions in Allende, Murchison, and Leoville indicate that they are found in many phases in high-temperature inclusions. El Goresy *et al.* (1978) observed nuggets of refractory trace metals in spinel, melilite, fassaite, and plagioclase. Wark and Lovering (1978) reported that the nuggets of refractory trace

metals occur mostly in melilite but also in spinel and on perovskite. Fuchs and Blander (1980) also reported these nuggets in fassaite, spinel, and melilite. Wark (1980) reported refractory trace metal nuggets in hibonite in inclusion 3643 in Allende. Grossman *et al.* (1977) reported refractory siderophile enrichments in two hibonite-bearing inclusions in the Murchison CM2 chondrite but no refractory trace metal nuggets were reported. Thus the literature reports appear to indicate that at least the larger refractory trace metal nuggets are concentrated in phases which nominally condense after corundum and hibonite but are seldom present in the highest-temperature condensates. We suggest doing a comprehensive survey for refractory trace metal nuggets in spinel–hibonite bodies in Murchison to see if the apparent rarity is real or a sampling or size effect.

#### DISCUSSION

From the above calculations it appears

probable that by the time the gas in the primitive solar nebula has become sufficiently supercooled to nucleate condensation centers, several different compounds, including the magnesium silicates forsterite and enstatite ( $\text{MgSiO}_3$ ), will be able to condense on the growing condensation center. Furthermore, an amorphous or glassy material instead of pure crystalline corundum is expected to condense because of energetic considerations. Once such a condensation center has grown beyond its critical size, then most condensable molecules which collide with it are likely to stick, forming a chemically heterogeneous mass of material. With the passage of time, if the condensate remains at an elevated temperature, internal annealing is likely to bring some order out of the chaos, but the resulting structure may well be quite complex.

Because of the great difficulty in creating new condensation centers, the importance of statistical fluctuations in the growth process is likely to be magnified, so that a condensation center, once formed, will feed from a considerable region of the surrounding gas and can thus grow to a substantial size. We suggest that many of the chondrules and high-temperature inclusions can be formed by condensation processes well inside the total evaporation front, from which they diffuse to fill the rest of the primitive solar nebula by turbulent transport.

To what sizes do we expect the condensation centers to grow? We estimated the growth rate of condensation centers by using the equation

$$dR/dt \approx w_j(n_j/n_i), \quad (15)$$

where  $R$  is the condensation center radius,  $n_j$  is the number density of the condensing constituent,  $w_j$  is the thermal velocity of the gaseous molecule which condenses, and  $n_i$  is the number density of the condensation center (Goldreich and Ward, 1973). Our estimate of condensation center growth rates due to condensation of  $\text{Mg(g)}$  and  $\text{SiO(g)}$  is

on the order of  $10^{-9}$  cm/sec. The condensation centers can be transported at velocities up to one-third of sound speed ( $\approx 10^5$  cm/sec). Near a radial distance of 1 AU in Fig. 6, the height of the shaded region is on the order of  $10^{12}$  cm. Transport over such a distance at the highest available speed requires times on the order of  $10^7$  sec, and in a diffusive process such as turbulent transport the residence time of a growing condensation is likely to be larger by a factor of a few. In  $10^7$  sec the condensation centers can grow to diameters on the order of 0.02 cm, and it should be noted that the radius grows linearly with time at a given degree of vapor supersaturation. Some centers will have smaller diameters while most will have larger sizes. The sizes of chondrules and inclusions in CM, CO, and CV chondrites are  $<0.05$  cm,  $<0.01$  to 0.04 cm, and 0.05 to 0.2 cm, respectively (Dodd, 1981). These size ranges are consistent with the expected sizes of the condensation centers.

Consider two different regions inside the total evaporation front. One region is in the radial outward direction from the point at which the total evaporation front crosses the midplane (at just less than 1 AU in Fig. 6). The other region lies above the total evaporation front where midplane is part of the total evaporation region. There is a conceptual difference between the possible condensation events in these two regions beyond the total evaporation front.

(1) At the midplane, condensation may occur when a parcel of gas moves radially outward past the total evaporation front. According to Fig. 6, it must move at least 0.2 AU for this to occur, and perhaps much more. One would expect any chondrules formed here to feed from the entire condensation sequence of the less volatile elements, since the component of the gravitational force perpendicular to the central plane of the nebula is very small and the condensates will drift only slowly relative to the gas.

(2) When a parcel of gas moves upward

across the total evaporation front, the perpendicular gravitational acceleration is much larger, and the temperature gradient is much steeper. If the growth of the condensation nucleus begins not too far inside the forsterite evaporation front, then the grain, when sufficiently large, may settle downward in the gravitational field, so that only the most highly refractory compounds condense on it. This is a possible source of high-temperature inclusions. Higher up from the midplane, additional condensation centers must be formed from gas now depleted in the most refractory elements, so that a different nucleation chemistry would prevail. Some types of chondrules may be formed this way.

In principle it should be possible to model the nebular processing of condensation centers by laboratory experiments. In practice, however, the possible variations in adjustable parameters make the design, execution, and analysis of meaningful experiments very difficult. Preliminary experiments on the nucleation and subsequent processing of condensation centers have been done by several groups, e.g., Nuth (1981) and Cohen (private communication, 1982). However, while these preliminary results are very interesting they do not adequately constrain the formation of inclusions and chondrules in the nebula because of the wide parameter ranges involved.

In reality, conditions are likely to be considerably more complicated than the above simple-minded scenario suggests. Nucleation requires the penetration of a parcel of totally evaporated gas to large distances beyond the total evaporation front. This penetration must occur within a highly turbulent medium, so that the parcel of gas is likely to become mixed with its surroundings after moving a pressure scale height. If the surrounding gas contains not completely evaporated interstellar grains, then these will act as nucleation sites for the supercooled gas. Such processes may be particularly important in the regions between the total evapo-

ration front and the forsterite evaporation front.

The almost complete evaporation of interstellar grains will concentrate the refractory trace metals present in the grains, such as Os and Pt, into tiny metal nuggets. Some of these nuggets will be stable against evaporation to temperatures greater than those at the total evaporation front. The composition of the nuggets present at any point will depend on the volatilities of the constituents which decrease in the order: Rh (most volatile) > Pt > Ru > Ir > Mo > Re > W > Os (least volatile) (Palme and Wlotzka, 1976). For example, pure Os nuggets will be stable against evaporation until 1674°K at  $10^{-6}$  bars and until 1747°K at  $10^{-5}$  bars. From Figs. 4 and 6 one can see that the evaporation front for osmium extends inward from the total evaporation front by about 0.2 AU at midplane.

The refractory trace metal nuggets which have been transported inward and have survived as a residue of the evaporation of agglomerates of interstellar grains will serve as nucleation centers for condensation of refractory trace metals and of supersaturated oxides between the total evaporation front and the forsterite evaporation front. Some nuggets may be almost totally evaporated and recondensed several times before incorporation into growing condensation centers. Others may be incorporated into condensation centers almost immediately. The refractory trace metal nuggets are not reported in all high-temperature inclusions. They appear to occur only in coarse-grained inclusions. We wonder if this selection effect is real or if tiny submicron nuggets are actually present in all inclusions. Cosmic abundance considerations indicate that the evaporation of interstellar grain aggregates on the order of 100  $\mu\text{m}$  in diameter will yield micron-diameter refractory trace metal nuggets. Evaporation of smaller grain aggregates, which should be much more common, will yield correspondingly smaller refractory trace metal nuggets. These smaller nuggets will also act as nu-

cleation centers for condensation. A thorough search for very small refractory trace metal nuggets in all high-temperature inclusions may prove rewarding.

It does appear possible that very large amounts of mass can be processed into chondrules and inclusions by these mechanisms, since turbulent transport within the primitive solar nebula should involve local shearing motions much faster than the bulk drift velocity of the gas toward the center of the nebula. Condensed bodies in the millimeter-size range will move quite readily with the gas wherever there are turbulent motions, which should diffusively distribute them throughout the bulk of the nebula. The turbulent motions can also easily sweep these small bodies to large distances away from midplane. Thin rims of materials of intermediate volatility may be deposited on these bodies in the course of the diffusion.

At a later stage in the development of the solar nebula, when the gas is sufficiently depleted to be optically thin, so that turbulent motions are no longer driven by thermal convection or meridional circulation currents, it is possible for material particles to sediment toward the midplane of the nebula. The rate of sedimentation is a function of particle size, with the larger particles falling more quickly toward midplane. When the central midplane mass density of condensed matter is high enough, Goldreich-Ward instabilities can take place, forming bodies of asteroidal size (Goldreich and Ward, 1973). We suggest that these instabilities take place at a time when the bulk of the chondrules and inclusions have precipitated, but only a much smaller fraction of the more finely divided material produced from the interstellar grains has reached the midplane region. In such a situation the mass ratio of chondrules to matrix material should be high in most asteroids and hence also in the meteorites derived from them.

#### ACKNOWLEDGMENTS

We are indebted to J. A. Smith and G. Weast for

constructing the large equation of state table that we used in these calculations. M.B.F. thanks R. Cohen for useful discussions of nucleation theory. Several people, including a referee, suggested that we extend the discussion that appeared in the preprint of this paper to deal with the effects of refractory trace metal nuggets, and in doing this we believe that we have improved the presentation. This research has been supported in part by NASA Grant NGR 22-007-269 in the areas of planetary geochemistry and geophysics and planetary atmospheres.

#### REFERENCES

- ADAMSON, A. W. (1967). *Physical Chemistry of Surfaces*, 2nd ed. Wiley-Interscience, New York.
- BLANDER, M., AND J. L. KATZ (1967). Condensation of primordial dust. *Geochim. Cosmochim. Acta* **31**, 1025-1034.
- BRUCE, R. H. (1965). Aspects of the surface energy of ceramics. I—Calculations of surface free energies. In *Science of Ceramics* (G. H. Stewart, Ed.), Vol. 2, pp. 359-381. Academic Press, New York.
- CAMERON, A. G. W. (1978). Physics of the primitive solar accretion disk. *Moon Planets* **18**, 5-40.
- DECAMPLI, W. M., AND A. G. W. CAMERON (1979). Structure and evolution of isolated giant gaseous protoplanets. *Icarus* **38**, 367-391.
- DODD, R. T. (1981). *Meteorites: A Petrologic-Chemical Synthesis*, pp. 38-53. Cambridge Univ. Press, London/New York.
- DRAINE, B. T., AND E. E. SALPETER (1977). Time-dependent nucleation theory. *J. Chem. Phys.* **67**, 2230-2235.
- DUGA, J. J. (1969). *Surface Energy of Ceramic Materials*. DCIC Report 69-2, Battelle Memorial Institute.
- EL GORESY, A., K. NAGEL, AND P. RAMDOHR (1978). Fremdlinge and Their Noble Relatives. *Proc. Lunar Planet. Sci. Conf. 9th*, 1279-1303.
- ELLIOTT, J. F., M. GLEISER, AND V. RAMAKRISHNA (1963). *Thermochemistry for Steelmaking*, Vol. II, pp. 654-658. Addison-Wesley, Reading, Mass.
- FEGLEY, M. B. (1980). *Chemical Fractionations in Solar Composition Material*. Ph.D. thesis, MIT.
- FEGLEY, M. B. (1982). Hibonite condensation in the solar nebula. *Lunar Planet. Sci. XIII*, 211-212.
- FUCHS, L., AND M. BLANDER (1980). Refractory metal particles in the Allende meteorite. *Proc. Lunar Planet. Sci. Conf. 11th*, 929-944.
- GOLDREICH, P., AND W. R. WARD (1973). The formation of planetesimals. *Astrophys. J.* **183**, 1051-1061.
- GROSSMAN, L., A. M. DAVIS, E. OLSEN, AND P. M. SANTOLIVUDO (1977). Chemical studies of condensates in the Murchison type 2 carbonaceous chondrite. *Lunar Planet. Sci. VIII*, 377-379.
- LIN, D. N. C., AND J. PAPALOIZU (1980). On the structure and evolution of the primordial solar nebula. *Mon. Not. Roy. Astron. Soc.* **191**, 37-48.
- LYNDEN-BELL, D., AND J. E. PRINGLE (1974). The evolution of viscous discs and the origin of the nebu-

- lar variables. *Mon. Not. Roy. Astron. Soc.* **168**, 603–637.
- MORFILL, G. (1981). Talk at Workshop on Star Formation, Aspen.
- NUTH, J. A. (1981). *Experimental and Theoretical Studies of Interstellar Grains*. NASA TM83883.
- PALME, H., AND F. WLOTZKA (1976). A metal particle from a Ca,Al-rich inclusion from the meteorite Allende, and the condensation of refractory siderophile elements. *Earth Planet. Sci. Lett.* **33**, 45–60.
- SALPETER, E. E. (1974). Nucleation and growth of dust grains. *Astrophys. J.* **193**, 579–584.
- SWALIN, R. (1972). *Thermodynamics of Solids*, 2nd ed. Wiley-Interscience, New York.
- TRIVEDI, B. M. P., AND J. W. LARIMER (1980). Some new mineral stability relations in cosmic systems. *Lunar Planet. Sci. XI*, 1165–1166.
- WARK, D. A. (1980). Allende CAI 3643—A layered record of protosolar nebula condensation. *Lunar Planet. Sci. XI* 1202–1204.
- WARK, D. A., AND J. F. LOVERING (1978). Refractory platinum metals and other opaque phases in Allende Ca-Al-rich inclusions (CAI's). *Lunar Planet. Sci. IX*, 1214–1216.